Biomaterials Science

ROYAL SOCIETY OF CHEMISTRY

PAPER

View Article Online
View Journal | View Issue

Check for updates

Cite this: *Biomater. Sci.*, 2024, **12**, 1228

Lubricity, wear prevention, and anti-biofouling properties of macromolecular coatings for endotracheal tubes†

Bernardo Miller Naranjo, [a,b] Michael Zollo, [c] Stephan A. Sieber [c] and Oliver Lieleg *[a,b]

Macromolecular coatings can improve the surface properties of many medical devices by enhancing their wetting behavior, tribological performance, and anti-biofouling properties – and covalent coatings produced from mucin glycoproteins have been shown to be very powerful in all those aspects. However, obtaining highly functional mucin glycoproteins is, at the moment, still a time-consuming process, which renders mucins rather expensive compared to other biomacromolecules. Here, we study a set of commercially available macromolecules that have the potential of substituting mucins in coatings for endotracheal tubes (ETTs). We present an overview of the different properties these macromolecular coatings establish on the ETT surface and whether they withstand storage or sterilization processes. Our study pinpoints several strategies of how to enhance the lubricity of ETTs by applying macromolecular coatings but also demonstrates the limited anti-biofouling abilities of well-established macromolecules such as hyaluronic acid, polyethylene glycol, and dextran. Based on the obtained results, we discuss to what extent those coatings can be considered equivalent alternatives to mucin coatings for applications on medical devices – their applicability does not have to be limited to ETTs, but could be broadened to catheters and endoscopes as well.

Received 5th December 2023,
Accepted 2nd January 2024

DOI: 10.1039/d3bm01985c

rsc.li/biomaterials-science

1. Introduction

When it comes to ensuring the supply of oxygen and anesthetics to patients that need to undergo certain medical interventions, endotracheal intubation remains the method of choice. This process, however, poses challenges for both, medical teams and patients alike: inserting the stiff, bent intubation tube into the trachea requires skill and practice; and even when this procedure is conducted by a trained expert, the hard endotracheal tube (ETT) slides across the soft tissue of the larynx and trachea during intubation and extubation. The resulting friction and tissue damage often leads to complaints and decreased acceptance among patients.[1] Here, modifying the ETT surface through coatings can be an interesting approach that might present a solution to these problems.[2–5] Indeed, coatings generated from different materials have already been used to modify the surfaces of many devices such as medical equipment and improved important properties including the tribological performance,[3,6–8] anti-biofouling behavior,[9,10] biocompatibility,[11] and hemocompatibility.[12]

In recent work, we introduced a setup that enabled us to perform *ex vivo* extubation tests on porcine tracheas, and we employed this setup to assess the functionality of mucin coatings generated on endotracheal tubes (ETTs).[13] Such mucins are large glycoproteins, which are physiologically present on all wet epithelia of mammalians. Here, they are responsible for a range of important tasks such as providing tissue hydration, lubricity, as well as anti-viral and anti-bacterial properties. When carefully purified from animal mucus, such mucins can also provide a similar range of important properties when used as components of biomaterials or coatings.[14] However, obtaining such purified mucins from porcine stomachs as described by Marczynski *et al.*[15] is still a comparably time-intensive and complex process that renders mucins more costly than other (bio)macromolecules, which are typically commercially available in large quantities and in purities that are sufficient for medical applications. Thus, we here asked if,

[a]*TUM School of Engineering and Design Department of Materials Engineering, Technical University of Munich (TUM), Boltzmannstraße 15, 85748 Garching, Germany. E-mail: oliver.lieleg@tum.de*
[b]*Center for Protein Assemblies (CPA) and Munich Institute of Biomedical Engineering (MIBE), Technical University of Munich (TUM), Ernst-Otto-Fischer Straße 8, 85748 Garching, Germany*
[c]*TUM School of Natural Sciences, Department of Bioscience, Chair of Organic Chemistry II Center for Functional Protein Assemblies (CPA), Technical University of Munich (TUM), Ernst-Otto-Fischer-Str. 8, Garching 85748, Germany*
† Electronic supplementary information (ESI) available. See DOI: https://doi.org/10.1039/d3bm01985c

in future applications of ETTs carrying macromolecular coatings, the mucin glycoprotein could be substituted with another macromolecule that improves the surface properties of ETTs in a similar manner as observed previously for mucin coatings.

When considering alternative macromolecules to create lubricating coatings on ETTs, both the size of those molecules and their ability to bind water are crucial parameters.[16,17] Thus, we here selected high-MW variants of the different macromolecular candidates which we explored as putative replacements for the very large mucin glycoprotein. Ideally, the selected macromolecules would also offer additional properties that go beyond friction reduction: when ETTs remain in a patient for extended time periods, biofouling events may occur which can lead to inflammation or increased problems during extubation. However, there is a boundary condition, which limited our choices: For us to be able to apply the same covalent coupling strategy, *i.e.*, carbodiimide chemistry (Fig. 1a), to generate the coatings (and this is desirable for better comparability), the macromolecules must contain primary carboxyl or amine. With all those considerations in mind, we here pre-selected (in addition to mucins) five macromolecules with different net charges as candidates for a comparative study: anionic hyaluronic acid (HA),[18,19] neutral polyethylene glycol (PEG) in two different molecular weights (100 kDa and 60 kDa), and the cationic macromolecules lysine dextran (L-Dex) and chitosan. HA, chitosan, and L-Dex all contain either primary carboxy or amino groups in the monomers; thus, applying carbodiimide-based coupling chemistry was no restrictive factor here. For PEG, however, neither group is present in the monomer. As a consequence, we employed a chemically modified variant (*i.e.*, amino-PEG).

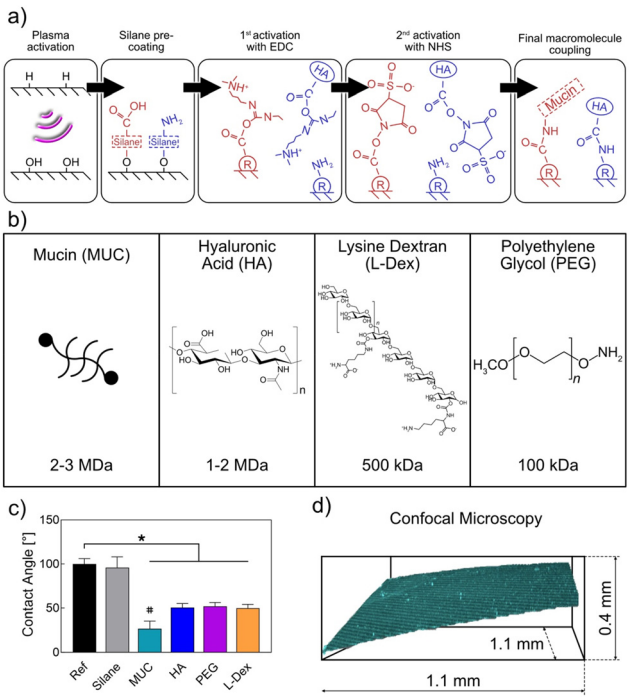

Fig. 1 Overview of the macromolecular coatings generated on endotracheal tubes (ETTs). (a) Coating process used to attach macromolecules to the endotracheal tube (ETT) surface. (b) Structural representation of the macromolecules used in this study. (c) Contact angles determined on different ETT samples. The bars represent the mean, and the error bars the standard deviation as calculated from at least n = 15 measurements determined on 9 independent samples. Significant differences towards uncoated ETT samples were determined *via* a two-sample t-test and are denoted with an asterisk (*). Significant differences among the four macromolecular coatings were detected *via* an ANOVA and Tukey *post-hoc* test and are marked with a rhombus (#). Differences were considered statistically significant for $p \leq 0.05$. (d) Confocal microscopy image of an ETT segment carrying a coating generated from fluorescently labelled HA.

Preliminary tests with those 6 macromolecules demonstrated that the larger PEG variant (PEG100) performed significantly better in enhancing the wettability of the ETT surface whereas the ability to reduce friction on the ETT surface was comparable for both PEG variants (ESI, section S1†). Coatings made from chitosan performed similarly well in both pre-tests as coatings generated from L-Dex. However, chitosan is only soluble at acidic pH and then requires a back-titration to (nearly) neutral pH to continue with the coating steps shown in Fig. 1a. From a future, application-driven point of view, this would add an extra processing step to the coating procedure, which is not ideal. Also, similar to mucin, chitosan is an animal product. Thus, chitosan coatings would not be suitable for the vegan community – yet this would be possible for L-Dex coatings. Based on those considerations, the set of 5 pre-selected, potential alternative macromolecules was reduced to three, and the main study was conducted with the list of molecules depicted in Fig. 1b.

The negatively charged biomacromolecule hyaluronic acid has been reported to have excellent water retention capabilities;[18,19] moreover, it exhibits anti-biofouling properties,[20] and can even act as an anti-inflammatory agent.[21] As HA is available in large amounts and in medical-grade purity, it is already widely used in the cosmetic and medical industry.[22–24] The uncharged, synthetic polymer polyethylene glycol (PEG) can bind large amounts of water as well.[25] PEG is highly biocompatible[26–28] and has been reported to reduce immunoreactivity,[29] which enables a broad range of biomedical applications. For instance, PEG has been employed as a component in coatings for medical devices, and such PEG-based coatings entailed an improved tribological performance of implants.[30] Moreover, these coatings can also provide medical devices with enhanced anti-biofouling properties, which underscores the great potential PEG holds for applications in biomedical engineering. Lysine dextran (L-Dex) is a synthetically generated macromolecule which is produced *via* the conjugation of the biocompatible polysaccharide dextran and the amino acid lysine.[31,32] Thus, it has free amine and carboxylate groups available for further conjugation and functionalization. L-Dex can bind several water molecules per monomer, which explains the good tribological performance observed for L-Dex coatings in technical settings.[33]

With this set of macromolecules, we here employed carbodiimide chemistry to generate covalent coatings on ETTs and compared their properties to those of mucin coatings. We studied if and to what extent the different coatings reduce fric-

tion and tissue damage on porcine tracheas, and we assessed the anti-biofouling properties of the coatings *via* cell/bacteria adhesion and lipid/protein deposition tests. Finally, we study the stability of the coatings towards storage and sterilization. Taken together, our results showed that, although mucin coatings remain superior, certain subsets of the manifold properties brought about by the mucin coating can also be provided by other macromolecules.

2. Results and discussion

Macromolecular coatings render the ETT surface hydrophilic

All ETT coatings studied here were generated from a set of macromolecules *via* carbodiimide chemistry (Fig. 1a and b) following strategies described in Winkeljann *et al.*[44] To verify the successful modification of the ETT surfaces, contact angle (CA) measurements were conducted. As shown in Fig. 1c, the contact angle of ultrapure water obtained on an uncoated ETT was ~100°, which represents a hydrophobic material. Upon application of any of the different coatings, this value was significantly reduced: In all cases, the coating process rendered the tubes hydrophilic. This result was in agreement with our expectation since we only selected hydrophilic macromolecules with good water binding capabilities to generate the coatings (ESI, section S2†). Still, the CA values obtained with the mucin coating was significantly lower than the values obtained for the other three coating variants. As another control, the CA was also determined on ETT samples, on which only the silane precoating was deposited. For those pre-coated ETTs, we found the virtually identical CA value as for uncoated ETTs. Taken together, this allowed us to conclude that the observed hydrophilization of the ETT surfaces was indeed a result of having successfully established the envisioned macromolecular coatings.

To confirm this finding, we labeled the macromolecules with fluorophores and imaged coatings generated from such labeled polymers using confocal microscopy. Whereas this method does not necessarily provide an accurate measurement of the coating thickness, it allows us to visually confirm the presence of the macromolecules on the ETT surface. As exemplarily shown in Fig. 1d for a coating generated from HA, we indeed were able to deposit a thin and even coating of this macromolecule with a thickness in the range of a few micrometers (ESI, section S3†).

Macromolecular coatings improve the tribological behavior of the ETTs

Having confirmed that the macromolecules were indeed successfully attached to the ETT surface, we next studied the effect the coatings have on the tribological performance of the tubes. To do so, we conducted extubation experiments on fresh porcine tracheas purchased from a butcher. With this setup, we determined the work required to pull a previously inserted ETT (see Methods) out of the trachea and compared the obtained result for ETTs carrying different coatings. Importantly, for all coating variants, we observed a significant reduction in the work required for extubation (Fig. 2a); in other words, all coatings were able to reduce friction between the ETT surface and the trachea tissue.

We further explore this result by comparing the lubricity provided by the different coatings. To do so, we conduct friction measurements directly on the coatings using a commercial rheometer equipped with a tribology unit and a steel-on-3-pins geometry. Fig. 3a and b show the friction coefficients obtained at a sliding speed of 15 mm s^{-1}, which corresponds to the pulling velocity used in our extubation experiments (for full speed sweeps, please refer to the ESI, section S4†). For all four coating variants, we observe a clear reduction in the friction coefficient compared to uncoated ETT samples. Again, this was to be expected as a key selection criterion we used when choosing the set of macromolecules was their capability to bind large amounts of water: the relevant mechanism that enables coatings to provide lubricity is hydration lubrication. Macromolecules immobilized onto the ETT surface can bind water molecules, which helps to separate the friction partners through a thin but robust layer of water that facilitates the sliding movement of both surfaces.[16,17]

However, a good sliding performance does not necessarily imply that the biological surface does not suffer from wear generation in response to the tribological challenge. Thus, to directly assess the ability of the coatings to reduce tissue damage, we conducted a Trypan Blue (TB) staining at two time points, *i.e.*, before and after the extubating process was conducted (see Methods). As TB is only taken up by cells that possess a damaged cell membrane, a blue staining result indicates local cell damage. With the double staining performed here, the first round of staining quantifies the initial degree of tissue damage present on the trachea sample, whereas the second round of staining and the increase in the blue staining signal resulting thereof represents the additional damage inferred by the extubation process. To quantify this increase in TB staining, image analysis was performed as described in detail in earlier work (ESI, section S5†).[13] The results obtained from this image analysis are summarized in Fig. 2b and show that, indeed, all the macromolecular coatings we tested here can significantly reduce the tissue damage caused by the extubation process – and with similar efficiency.

Selected macromolecular coatings mitigate biofouling events on the ETTs

During their clinical use, ETTs come in direct contact with lung tissue. This can trigger biofouling events which, in turn, may compromise the functionality of the device. Such biofouling events include the colonization of the ETT surface by cells/bacteria or the deposition of lipids/proteins present on the surface of the trachea. Previously, we have shown that mucin coatings can successfully suppress those biofouling events.[7,13] However, it remains to be shown if the alternative macromolecular coatings we study in this work are similarly potent in mitigating those undesired processes. Thus, in a next step, we studied the ability of the different coatings to prevent or

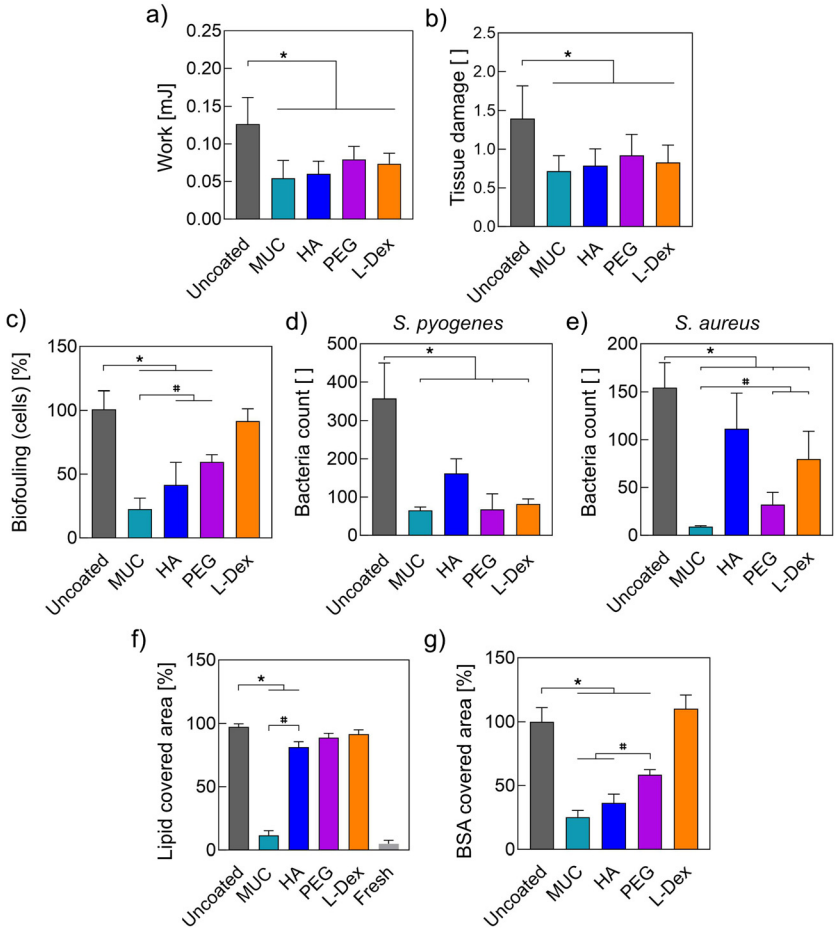

Fig. 2 Overview of the different functionalities brought about by the coatings. (a) Work necessary for extubation as determined at a defined sliding speed of 15 mm s^{-1}. (b) Tissue damage caused by the process of extubation (assessed *via* Trypan Blue (TB) staining). (c) Cellular and (d and e) bacterial colonialization of different ETT surfaces. Biofouling of ETT surfaces by (f) lipids and (g) proteins (BSA). Data shown denotes average values and error bars represent the standard deviation as calculated from at least n = 5 independent samples (n = 8) for subfigures (a–c), n = 9 for subfigures (d–e), and n = 5 for subfigures (f–g). Asterisks (*) and rhombi (#) denote significant differences towards uncoated ETTs (analyzed *via* a 2-sample t-test) and among different coatings (tested *via* an ANOVA and Tukey *post-hoc* test), respectively (based on a p-value of p = 0.05).

reduce the colonization of ETT surfaces by eukaryotic cells (HeLa cell line).

First, we tested whether the components used to generate the coatings or the ETTs themselves negatively affect the viability of HeLa cells. Importantly, by conducting a leaching assay, we found that neither the ETT material itself nor any of the coatings compromised the viability of cells incubated with the respective leaching medium (ESI, section S6†). Then, we directly seeded HeLa cells onto different ETT samples and quantified the number of adsorbed cells by determining their collective metabolic activity *via* a WST-1 assay (Fig. 2c). The obtained results agreed with a qualitative assessment of this cellular biofouling *via* a live/dead staining (ESI, section S6†) and showed that, indeed, the different coatings reduce ETT colonialization by cells with different efficiencies: whereas L-Dex coatings failed in reducing cell attachment, all other coatings generated from either mucin, HA, or PEG significantly reduced cellular biofouling compared to uncoated tubes, *i.e.*, by 75%, 60%, and 40%, respectively.

In part, these results might be explainable by electrostatic interactions. As cell membranes are negatively charged,[34] electrostatic repulsion effect can be expected when cells are seeded onto surfaces carrying anionic macromolecules. This is the case for HA, which carries a negative charge on each monomer, and mucins, where the glycans in the middle section of the glycoprotein convey an overall polyanionic character to the macromolecule. In contrast, coatings generated from the cationic L-Dex should entail attractive electrostatic interactions between the anionic cell membrane and the cationic coating, which might even facilitate the surface colonization by cells. PEG is an uncharged polymer but has been reported to be biologically inert, so that it does not promote cell adhesion or proliferation.[35,36] And indeed, our results were consistent with this notion. Nevertheless, here, neutral PEG coatings were less efficient in reducing cell adhesion than the anionic HA or mucin coatings – and the difference between PEG coatings and mucin coatings was significant.

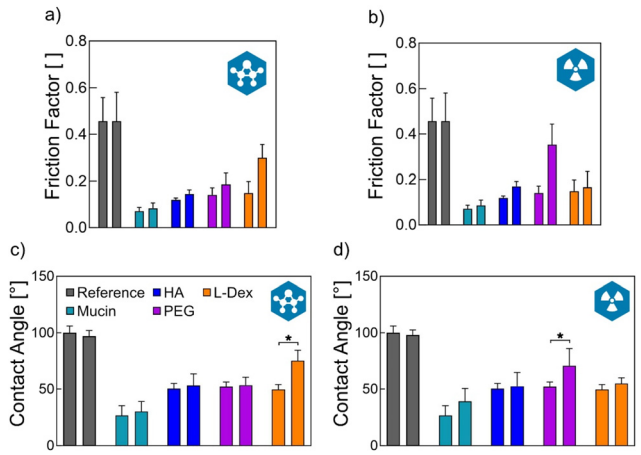

Fig. 3 Effect of sterilization processes on the coated ETTs. The friction factor (a and b) determined directly on the coatings and contact angle (CA) measurements (c and d) were chosen to assess the presence and functionality of the coatings on the endotracheal tube (ETT) surface. Two sterilization methods are compared: ethylene oxide fumigation (a and c) and gamma irradiation (b and d). Bars represent the mean and the error bars the standard deviation as calculated from $n = 3$ measurements conducted on independent sample sets for the friction factor and from $n \geq 15$ measurements on 9 independent samples for the CA. Asterisks (*) denote significant differences determined *via* a two-sample *t*-test based on a *p*-value of $p = 0.05$.

There are several factors that seem to affect the anti-biofouling performance of a coating, and those factors include the zeta potential and the wettability of the created surface, its topography, and its mechanical properties.[37–39] Some of those factors – but not all – can be adjusted by varying the coating thickness. And, indeed, there are reports in the literature suggesting that the coating thickness can influence the physical and biological properties of a coating.[40] Thus, a larger PEG variant than the PEG100 used here might have a stronger effect in reducing the cell attachment to the ETT surface. Still, for the carbodiimide-based coating strategy employed here, the PEG100 variant was the largest commercial option we could find that carries the necessary amino- (or carboxy-) modification.

Another possible source of complication is the bacterial colonization of ETTs, which can lead to serious infections. To assess the ability of the different macromolecular coatings to reduce bacterial adhesion, we selected three different model bacteria: *S. pyogenes*, which often colonizes the throat mucosa; *S. aureus*, which causes skin and respiratory infections; and *P. aeruginosa*, which causes lung infections. Coated ETT samples were incubated in overnight cultures containing one of these bacteria; afterwards, the ETT samples were rinsed, and microscopy images were obtained to determine the number of adherent bacteria. As summarized in Fig. 2d,e, we obtained the strongest effect for *S. pyogenes*. Here, only HA coatings were not successful in significantly reducing the number of adhering bacteria. For *S. aureus*, mucin-, PEG-, and L-Dex coatings could significantly reduce bacterial adhesion – but also here, HA coatings failed to do so. In similar tests conducted with the strain *P. aeruginosa* (Fig. S7†), all coatings failed to mitigate bacterial adhesion – even the mucin coatings. The latter, however, is not surprising as *P. aeruginosa* is a mucoadhesive strain that can bind to mucins.

Of course, not only a colonization by eukaryotic and prokaryotic cells but also an adsorption of molecules onto the ETT surface can alter the surface properties of the tube and thus affect its behavior. In previous studies, we observed that mucin coatings can also very efficiently reduce lipid deposition events onto medical devices such as contact lenses and ETTs,[7,13] and we reproduced this behavior here (Fig. 2f and ESI, section S8†). Different from mucin coatings, coatings generated from PEG and L-Dex failed to prevent or even reduce the adsorption of lipids to the ETT surface, and HA coatings showed only a weak effect. This result was somewhat surprising but demonstrated that the mechanism responsible for the lipid-repelling properties of mucins has yet to be deciphered. Nevertheless, it also underscored the superior anti-biofouling properties of mucins compared to that of other biopolymers.

Interestingly, the mucin coating also outperformed most other coating variants when we tested the coatings' ability to mitigate protein adsorption to the ETT surface (Fig. S9†). Here, ETT samples were coated and incubated in PBS containing 0.1% (w/v) of the model protein bovine serum albumin (BSA). The obtained results (Fig. 2g) show that coatings generated from mucin, HA, and PEG significantly reduced the adsorption process of BSA. In contrast, L-Dex coatings failed to do so. This can be explained as BSA has an isoelectric point around pH 5 and thus is negatively charged at neutral pH, which gives rise to electrostatic attraction between the BSA molecules and the L-Dex coating. Similarly, electrostatic repulsion might explain why the coatings assembled from the anionic mucin and HA outperformed the coatings generated from neutral PEG.

Macromolecular coatings are stable during storage and maintain their lubricity after sterilization

When considering their envisioned use as a medical product, the ETTs would typically be stored for a while after the coating has been applied, and the applied coating needs to be stable during such a storage period. And indeed, we here found that neither the wettability nor the lubricity of coated ETTs were decreased over time: up to 8 weeks, all coatings remained stable during both, wet and dry storage (ESI, section S10†). This positive outcome is a direct result of the covalent coupling procedure used here attach the macromolecules to the ETT surface.

Of course, all medical devices need to be sterilized before being used on human patients. It is therefore a crucial requirement for the coated ETTs to maintain their functionality after such a sterilization process. Here, we tested the stability of the different coatings towards two common sterilization methods, *i.e.*, ethylene oxide (EO) fumigation and gamma irradiation. The presence of the coating was tested *via* contact angle measurements whereas the lubricating functionality of the coating was quantified by measuring the friction factor directly on the coating (for full friction curves, refer to SI, section S4†).

Table 1 Overview of the properties of different macromolecular ETT coatings generated from either mucin (MUC), hyaluronic acid (HA), polyethyleneglycol (PEG), or lysine-dextran (L-Dex). The different colors denote: red = unsatisfactory performance, yellow = satisfactory performance; green = very good performance

		MUC	HA	PEG	L-Dex
Wettability					
Friction reduction					
Tissue damage prevention					
Anti-biofouling					
	Cells				
	Bacteria				
	Lipids				
	Proteins (BSA)				
Sterilizability					
	EO				
	γ-irradiation				
Long-term stability					
	Dry storage				
	Wet storage				

Fig. 3c and d show that the hydrophilization of the ETT surface provided by the coatings was very well maintained in most cases. It was only significantly compromised for the L-Dex coating when treated with EO and for the PEG coating when treated with gamma radiation. The latter corresponds to previous reports, which showed that PEG is indeed negatively affected by gamma radiation.[41] When testing the lubricity of sterilized coatings, our results were in full agreement with our CA data: we only observed increased friction coefficients for those two coating/treatment combinations, where we also detected alterations in the hydrophilic properties of the sterilized ETT surface. Taken together, we concluded that, for each coating variant tested here, at least one standard sterilization method can be found (either EO fumigation or gamma irradiation) that maintains the hydrophilizing and lubricating effect the coatings have on the ETT surface.

In summary, we here compared different macromolecular coatings generated on commercial ETTs and analyzed their ability to reduce friction and tissue damage, to mitigate biofouling events, and to maintain their properties after storage and sterilization. Our results showed that, depending on the macromolecule selected, the coating properties do differ (for an overview, see Table 1): whereas, in terms of friction reduction and prevention of tissue damage during extubation, all four coatings performed similarly well, the anti-biofouling properties of mucin coatings turned out to be clearly superior to those observed for the other macromolecular coatings.

3. Conclusion

For such scenarios, where only short-term intubation is needed, any of the macromolecular coatings studied here could be a good choice to improve the surface properties of ETTs. However, if good anti-biofouling properties are required in addition to lubricity (and this would be the case when an ETT remains in a patient for longer time periods), mucin coatings would still the best choice. Then, also cell/bacteria colonization and lipid/protein deposition can be very efficiently prevented as well. In principle, it seems possible that a chemically modified version of either HA or PEG might be able to provide similarly strong anti-biofouling properties as mucins do; however, to be able to generate such an enhanced variant of those commercially well available macromolecules, it is paramount to better understand how mucins achieve those anti-biofouling properties and which chemical motifs from the highly complex glycoprotein are required for this. Until then, further improving existing purification strategies to obtain highly functional mucins in both, large quantity and medical-grade purity, seems to be the more feasible strategy.

4. Experimental section/methods

Macromolecules

Mucin MUC5AC (MUC). The glycoprotein mucin has excellent lubricating properties. We purify this macromolecule from porcine stomachs by following multi-step process (see below). For those lab-purified mucin glycoproteins (which occur as oligomers), the estimated molecular weight is 2–3 MDa.[42]

Hyaluronic acid (HA). HA is well known for its capability to bind large amounts of water. The HA variant used in this study was purchased from Biosynth AG (St. Gallen, Switzerland) and has a molecular weight of 1–2 MDa.

Lysine dextran (L-Dex). This synthetically produced macromolecule has many binding sites for water, so that it holds the potential of enhancing lubrication when used as a coating. The L-Dex used for this study was purchased from TdB Labs (Uppsala, Sweden) and has a molecular weight of 500 kDa.

Polyethylene glycol (PEG). PEG is widely used for many applications including problems in biomedical engineering. One important property of PEG is its ability to bind water. The PEG variant we use here was purchased from Rapp Polymere GmbH (Tübingen, Germany) and has an average molecular weight of 100 kDa.

Mucin purification

Porcine gastric mucin was purified as described in Marczynski *et al.* (2022). In brief, gastric mucus was harvested from fresh porcine stomachs purchased at a local slaughterhouse on the day of processing. The pig stomachs were cut open and gently rinsed with water from the tap. Then, the inner surface of the tissue was scraped to collect the mucus. The obtained mucus was diluted 5-fold in 10 mM sodium phosphate-buffered saline (PBS, pH 7.0) enriched with 170 mM NaCl and 0.04% (w/v) sodium azide, and stirred at 4 °C overnight. The homogenized mucus was subjected to four consecutive filtering steps by passing the mucus through metal grids with mesh sizes of 1 mm, 500 μm, 200 μm, and 125 μm, respectively. Afterwards, the mucin glycoproteins were isolated from the other mucus constituents by size exclusion chromatography (SEC) using an ÄKTA purifier system (GE Healthcare, Munich,

Germany) equipped with an XK50/100 column packed with Sepharose 6FF resin (GE Healthcare). The collected mucin fractions were pooled and the NaCl concentration was increased to 1 M. Then, this mucin solution was dialyzed against ultrapure water and concentrated by cross-flow filtration (MWCO: 100 kDA; QuixStand benchtop crossflow system, GE Healthcare) equipped with a hollow fiber module with a molecular weight cut-off of 100 kDa (Xampler Ultrafiltration Cartridge, GE Healthcare). Finally, the concentrate was lyophilized and stored at −80 °C until further use.

Coating process

Lab-purified porcine gastric mucins were covalently bound to the outer surface of commercial endotracheal tubes (ETTs, Super Safetyclear, made from polyvinylchloride (PVC), 10.0 mm, CH40, Radecker Notfallmedizin Ammerbuch/Entringen, Germany) using a procedure described in Winkeljann *et al.*[43] In brief, the ETTs were removed from their sterile packaging and carefully cut into pieces of ∼15 cm in length. After rinsing in 80% (v/v) ethanol and ultrapure water, the tubes were plasma-activated in a plasma oven (SmartPlasma 2.0, plasma technology GmbH, Herrenberg-Gültstein, Germany) by exposing them to atmospheric plasma at a pressure of 0.4 mbar and an intensity of 30 W for 90 s. In this step, the methyl groups on the surface were substituted with hydroxyl groups. Then, the coupling agent *N*-[(3-trimethoxysilyl)propyl]-ethylenediamine triacetic acid trisodium (TMS-EDTA, abcr GmbH, Karlsruhe, Germany) was used to prepare the sample surface for the following carbodiimide coupling steps. TMS-EDTA was diluted to a concentration of 1% (v/v) in 10 mM acetate buffer (pH 4.5), and the samples were incubated in this solution at 60 °C for 5 h. After this step, the samples were dipped into isopropanol (>99.5% (v/v)) and washed in 96% (v/v) ethanol for 1 h on a rolling shaker (70 rpm, RS-TR 05, Phoenix Instrument GmbH, Garbsen, Germany). Then, the samples were incubated at 110 °C to stabilize the siloxane bond. Afterwards, the ETTs were incubated on a rolling shaker (70 rpm) where they were immersed in 100 mM MES buffer (pH 5.0) containing 5 mM EDC and 5 mM sulfo-NHS at room temperature for 30 min. In a final step, mucins were dissolved in 1x Dulbecco's phosphate-buffered saline (DPBS; Lonza, Verviers, Belgium) at a concentration of 0.1% (w/v), and the ETTs were incubated in the mucin solution at 4 °C for 12 h. Finally, the coated tubes were gently washed in 80% (v/v) ethanol and stored in 20 mM HEPES (4-(2-hydroxyethyl)-1-piperazineethane-sulfonic acid) buffer (pH 7) until further use.

Contact angle measurements

To compare the wetting behavior of ETTs coated with the different macromolecules, contact angles (CAs) were determined on small rectangular (5 mm x 16 mm) pieces cut from the ETTs. A commercial drop shape analyzer device (DSA25S, Krüss GmbH, Hamburg, Germany) was used to perform these measurements. Uncoated samples were washed with 70% (v/v) ethanol and rinsed with Millipore water; coated samples were removed from the storage buffer (see above). Before conducting measurements, all samples were dried for ∼3 s using oil-free pressurized air (Aero Duster 105/2). Then, a 2 μL droplet of ultrapure water was placed onto each sample (which was placed with its long axis perpendicular to the light path), and lateral images were captured with a high-resolution built-in camera (acA1920. Basler, Ahrensburg, Germany).

Rotational tribology

To test the tribological performance of the macromolecular coatings, rotational tribology measurements were conducted on a commercial shear rheometer (MCR 302, Anton Paar, Graz, Austria) equipped with a tribology unit (T-PTD 200, Anton Paar). Rectangular samples (6 mm x 14 mm) were cut from fresh ETTs such that the long side of those pieces was parallel to the longitudinal axis of the ETTs. A steel sphere with a diameter of 12.7 mm (1.4301, S_q < 0.2 μm, Kugel Pompel, Vienna, Austria) was chosen as a friction partner. Tests were conducted in a ball-on-3-plates geometry using a commercial sample holder (Anton Paar). A logarithmic speed ramp from 100 mm s^{-1} to 0.001 mm s^{-1} was performed while applying a constant normal force of F_N = 6 N, and the resulting friction coefficient was evaluated at 39 distinct speed levels for 10 s each. For each measurement, 600 μL of buffer (4-(2-hydroxyethyl)-1-piperazineethanesulfonic acid = HEPES, 20 × 10^{-3} M, pH 7.0) were used as a lubricant.

Tracheal sample preparation

Fresh porcine trachea samples were obtained from a local slaughterhouse. Adjacent tissue was carefully removed, and special care was taken not to damage the inner walls of the tracheas. Then, the trachea samples were rinsed in 1x phosphate buffered saline (PBS) to remove residual mucus. Afterwards, the tracheas were slit open longitudinally and two samples with defined dimensions (5 cm in length and 4 cm in width) were cut from each trachea.

Extubation tests

To compare the different coatings in terms of their ability to reduce tissue damage generation, a setup previously described was used to conduct controlled extubation experiments.[13] This extubation device comprises a linear motor stage with a built-in control unit, an air bearing that creates an air cushion so the internal friction of the device is minimized, and an S-shaped force sensor, which (in combination with a 24-Bit amplifier) allows for force measurements with a resolution in the range of 2 mN. Additionally, an optical encoder (model LPD3806, Fockety, People's Republic of China) was integrated with a microcontroller (Arduino UNO R3, Somerville, MA, United States of America) to measure the distance traveled by the shaft of the device.

For each extubation experiment, a 15 cm long piece of ETT was cut and straightened by inserting a threaded shaft (M4) and two plugs with M4 threads at either end of the ETT segment. One of the plugs was connected to a hook, so it could be attached to the linear motor. The trachea samples

were slit open along their longitudinal axis and the straightened ETTs were gently inserted. They were then placed into a custom-made PDMS cushion and the whole construct was clamped using two aluminum pieces. To ensure that all trachea samples are loaded with comparable normal pressure (~16 kPa), a force sensor (ZD10-100, Walfront Electronics, Shenzhen, People's Republic of China) was placed between the PDMS cushion and the lower half of the aluminum casing.

The control unit of the motor was programmed to drive out 90 mm at a speed of 15 mm s^{-1}, then wait in that position for 5 s (to be able to connect the tube to the motor), and then pull the ETT out of the trachea at a speed of 15 mm s^{-1}; during this last phase, force and distance signals were recorded and evaluated.

Biofouling tests

Cell colonization. To study the ability of the coatings to suppress sample colonization by eukaryotic cells, the cell line HeLa was selected as a model. HeLa cells were maintained in standard medium (DMEM supplemented with 5% FCS and 1% penicillin/streptomycin) at 37 °C and 5% CO_2.

The cell attachment efficiency to different ETT samples was assessed by a water-soluble tetrazolium salt (WST-1, 5015944001, Sigma-Aldrich) assay. First, cylindrical samples were cut from freshly unpacked ETTs and coated, then disinfected by dipping them into 96% (v/v) ethanol and placed into 48-well plates with the concave side facing up. Then, HeLa cells were harvested, and 50 000 cells were seeded onto each sample in such a way that the cells remain on the concave side of the sample. After an incubation time of 4 h, which should give the cells enough time to attach to the ETT surface, the samples were gently rinsed with sterile PBS, placed in fresh wells, and 250 μL of a WST-1 solution were added to each of the samples. After 1 h of incubation, 100 μL of the WST-1 solution were withdrawn from each well and transferred into a new 96-well plate to conduct absorbance measurements at 450 nm with a plate reader (SpectraMax® ABS Plus, Molecular Devices, San Jose, USA). The measured absorbance values were then normalized to those obtained for uncoated tubes used as a control group.

Bacterial attachment. The ability of the coatings to reduce bacterial colonization of the ETT surface was tested using three bacterial model organisms that are of general clinical relevance: *S. aureus*, S. pyogenes, and *P. aeruginosa*, as described in previous work.[43] For all strains, overnight cultures were produced at 37 °C and 5% CO_2 using different media for bacterial growth, as follows: *S. aureus* (strain USA300) was cultivated in Lysogeny Broth (Carl Roth) supplemented with 0.1% dibasic potassium phosphate (Acros Organics, Massachusetts, United States of America) and incubated under shaking, S. pyogenes (strain ATCC 700 294) in Brain Heart Infusion Broth (Carl Roth) without shaking, and *P. aeruginosa* (strain PAO1) in pure Lysogeny Broth under shaking. The bacteria were then diluted to an optical density (OD600) of 0.2. Substrate samples with a diameter of 6 mm were stamped from fresh ETTs and then were coated following the procedure described in the main article. A set of coated and uncoated samples was placed into wells of a 96-well-plate (one sample per well, $n = 3$ samples per condition). Then, 100 μL of the respective bacterial solution were pipetted into each well and incubated for 1.5 h at 37 °C and 5% CO_2. After incubation, unattached bacteria were removed together with the supernatant, and the samples were rinsed 2 times with sterile PBS (200 μL). Then, images of the ETT samples ($N = 3$ images per sample) were captured at 40× magnification using a microscope (Zeiss Axiovert, Zeiss, Oberkochen) equipped with a Zeiss Axiocam 305 color camera (Zeiss), and the number of adherent bacteria was quantified using the software ImageJ (version 2.3.0/1.53q, 2021). In detail, the "find maxima" command was used with the "exclude edge maxima" and "light background" options being activated. The noise tolerance was set individually for every image. To make sure that all samples are treated equally, exposure times and light intensity were defined for the first sample and then kept unchanged for all samples.

Lipid adsorption. The anti-biofouling properties of coatings were studied *via* lipid deposition tests as conducted previously in Miller Naranjo *et al.* For these tests, cylindrical samples with a diameter of 7 mm were stamped out of fresh ETTs and coated as described above. Dipalmitoyl-phosphatidylcholine (DPPC, Avanti Polar Lipids, AL, USA) was used as a model molecule for the lung surfactant. Cool ultrapure water (6–10 °C) was used to prepare a solution containing 0.05% (w/v) DPPC and 2.5% (w/v) tetrahydrofuran (Sigma-Aldrich, St. Louis, MO, USA).

After dipping the ETT samples in ultrapure water for 20 s, they were submerged into the lipid solution for 60 min. Subsequently, they were rinsed in ultrapure water for 10 s, and images of the rinsed samples were acquired on a black background using a digital system camera (Canon EOS M50 Mark II, Canon, Canon Inc., Tokyo, Japan). Afterwards, the images were analyzed with the software ImageJ (version 2.3.0/1.53q, 2021) as follows: to avoid artefacts arising from reflection effects, an area of interest was marked while leaving out the border of the sample. Then, the images were converted into 32-bit grayscale and a threshold filter (high-pass; threshold value: 150) was employed to find sample segments covered with lipids. Finally, the total area covered with lipids was compared to the area of the whole sample.

Protein adsorption. The ability of the coatings to reduce protein adsorption to the ETT surface was studied as follows: Bovine serum albumin (BSA portion V, Sigma Aldrich) was dissolved at a concentration of 0.1% (w/v) in PBS. Then, cylindrical ETT samples were incubated in the BSA solution at room temperature (RT) for 60 minutes while gently shaking. After incubation, the samples were rinsed with Millipore water and dried at RT for 10 min. After those steps, samples, onto which the protein adhered, had partially turned opaque (white). Then, images of the incubated samples were acquired using a digital camera (Canon EOS M50 Mark II, Tokyo, Japan) and analyzed using the software ImageJ (version 2.3.0/1.53q, 2021). For this image analysis step, we manually marked the circular area of interest representing the round ETT sample (diameter

~7 mm). The images were then converted into a 32-bit grayscale, and a high-pass filter was applied using a threshold value of 150. The opaque area on the ETT sample was then compared to the full area of the sample to determine the fraction of the ETT sample surface covered with protein.

Stability tests

To be able to be used in the human body, medical products need to be sterile. To obtain sterile samples carrying macromolecular coatings, rather than working in a sterile environment when creating the coatings, we apply sterilization processes to samples generated under non-sterile conditions. To achieve this, there are several methods available, such as steam sterilization (autoclaving), chemical treatment, and exposure to radioactive radiation. Here, we test the stability of the generated coatings towards two commonly used sterilization methods: ethylene oxide (EO) fumigation and γ-irradiation. For sterilization treatment, the coated ETT samples were stored in sterilization bags (Medi Pack GmbH, Mönchengladbach, Germany) and standard processes offered by the company steripac GmbH (Calw, Germany) were applied as described below.

Ethylene oxide fumigation. The samples were exposed to EO gas (average concentration of 700 mg L^{-1}) for 5 h at 610 mbar of pressure and at 45 °C.

γ-Irradiation. To meet the standards dictated by the norms EN ISO11137-1, EN ISO13485 and EN ISO 9001, the ETT samples were exposed to a dose of 25–50 kGy in a pallet irradiator of the type JS9000.

After each of those sterilization procedures, the effect of the respective process on the coatings was studied *via* CA and friction measurements using the protocols described above. With the same two methods, we also investigated the influence of the following physico-chemical challenges on the coatings.

Storage. Rectangular samples were cut from fresh PVC ETTs and coated according to the procedure described above. To test the long-time stability of the coatings, coated ETT samples were stored either in PBS at 37 °C or in a dry state at room temperature (~22 °C). After 1, 4, and 8 weeks, CA and tribology measurements were conducted to determine the remaining degree of functionality of the coatings after storage.

Statistics

Statistical tests were conducted to find significant differences in all data sets except for the long-term stability and the steel-on-PDMS friction measurement (here, the sample size was n = 3 and thus too small to apply a robust statistical analysis). A Shapiro–Wilk test was used to test for normal data distribution, and a two-sample F-test was employed to test for equality of variances. A two-sample t-test was used to test for significant differences between data sets with normal distribution and equal variances. Data sets with normal distribution and non-equal variances were analyzed with a Welch's t-test. For data sets, which were not normally distributed, a Wilcoxon-Mann–Whitney test was applied. These statistical analyses were all performed employing the program Matlab (version 2022a, Mathworks, MA, USA).

To find differences between the different coatings, one-way ANOVA tests were conducted on data sets with normal distribution. Data sets, which were not normally distributed, were tested using a Kruskal–Wallis-ANOVA test. Then, in either case, Tukey *post-hoc* tests were performed to identify which samples were significantly different. These tests were conducted using the software OriginPro (version 2023b, OriginLab Corporation, MA, USA). In all cases, differences were considered statistically significant if a p-value lower than 0.05 was obtained.

Author contributions

O. L. and B. M. N. designed the experiments. M. Z. conducted and analyzed the bacteria colonization experiments. B. M. N. acquired and analyzed all other data. The manuscript was written by B. M. N. and O. L. All authors gave approval to the final version of the manuscript.

Conflicts of interest

The authors declare no conflict of interest.

Acknowledgements

This study was supported by the German Research Foundation (DFG) *via* grant LI-1902/15-1.

References

1 E. Servera, J. Sancho, M. J. Zafra, A. Catalá, P. Vergara and J. Marín, Alternatives to endotracheal intubation for patients with neuromuscular diseases, *Am. J. Phys. Med. Rehabil.*, 2005, **84**(11), 851–857.

2 S. Ito, N. Shimohata, S. Iwanaga, W. Ito, M. Ohba, M. Mochizuki, T. Nakagawa, S. Suzuki, N. Sasaki and I. Koshima, Prevention of intubation-induced mucosal damage using a tube coated with 2-methacryloyloxyethyl phosphorylcholine polymer, *Eur. J. Anaesthesiol.*, 2012, **29**(2), 100–104.

3 M. H. Bai, B. Zhao, Z. Y. T. Liu, Z. L. Zheng, X. Wei, L. Li, K. Li, X. Song, J. Z. Xu and Z. M. Li, Mucosa–Like Conformal Hydrogel Coating for Aqueous Lubrication, *Adv. Mater.*, 2022, 2108848.

4 Y.-P. Li, W. Liu, Y.-H. Liu, Y. Ren, Z.-G. Wang, B. Zhao, S. Huang, J.-Z. Xu and Z.-M. Li, Highly improved aqueous lubrication of polymer surface by noncovalently bonding hyaluronic acid-based hydration layer for endotracheal intubation, *Biomaterials*, 2020, **262**, 120336.

5 B. Zhao, Y.-P. Li, Q. Wang, Y. Ren, Z.-L. Zheng, M.-H. Bai, J.-C. Lv, K. Li, J.-Z. Xu and Z.-M. Li, Ultra-slippery, nonirritating, and anti-inflammatory hyaluronic acid-based

coating to mitigate intubation injury, *Chem. Eng. J.*, 2022, **427**, 130911.
6 R. Wang, Y. Xiong, K. Yang, T. Zhang, F. Zhang, B. Xiong, Y. Hao, H. Zhang, Y. Chen and J. Tang, Advanced progress on the significant influences of multi-dimensional nanofillers on the tribological performance of coatings, *RSC Adv.*, 2023, **13**(29), 19981–20022.
7 C. A. Rickert, B. Wittmann, R. Fromme and O. Lieleg, Highly transparent covalent mucin coatings improve the wettability and tribology of hydrophobic contact lenses, *ACS Appl. Mater. Interfaces*, 2020, **12**(25), 28024–28033.
8 C. A. Rickert, I. Piller, F. Henkel, R. Fromme and O. Lieleg, Multifunctional glycoprotein coatings improve the surface properties of highly oxygen permeable contact lenses, *Biomater. Adv.*, 2023, **145**, 213233.
9 Z. K. Zander and M. L. Becker, *Antimicrobial and antifouling strategies for polymeric medical devices*, ACS Publications, 2018.
10 I. Francolini, C. Vuotto, A. Piozzi and G. Donelli, Antifouling and antimicrobial biomaterials: an overview, *APMIS*, 2017, **125**(4), 392–417.
11 M. N. Helmus, D. F. Gibbons and D. Cebon, Biocompatibility: meeting a key functional requirement of next-generation medical devices, *Toxicol. Pathol.*, 2008, **36**(1), 70–80.
12 M. C. Frost, M. M. Reynolds and M. E. Meyerhoff, Polymers incorporating nitric oxide releasing/generating substances for improved biocompatibility of blood-contacting medical devices, *Biomaterials*, 2005, **26**(14), 1685–1693.
13 B. Miller Naranjo, S. Naicker and O. Lieleg, Macromolecular Coatings for Endotracheal Tubes Probed on An Ex Vivo Extubation Setup, *Adv. Mater. Interfaces*, 2023, **10**(6), 2201757.
14 G. Petrou and T. Crouzier, Mucins as multifunctional building blocks of biomaterials, *Biomater. Sci.*, 2018, **6**(9), 2282–2297.
15 M. Marczynski, C. A. Rickert, T. Fuhrmann and O. Lieleg, An improved, filtration-based process to purify functional mucins from mucosal tissues with high yields, *Sep. Purif. Technol.*, 2022, **294**, 121209.
16 U. Raviv and J. Klein, Fluidity of bound hydration layers, *Science*, 2002, **297**(5586), 1540–1543.
17 U. Raviv, S. Giasson, N. Kampf, J.-F. Gohy, R. Jérôme and J. Klein, Lubrication by charged polymers, *Nature*, 2003, **425**(6954), 163–165.
18 K. Haxaire, Y. Marechal, M. Milas and M. Rinaudo, Hydration of hyaluronan polysaccharide observed by IR spectrometry. II. Definition and quantitative analysis of elementary hydration spectra and water uptake, *Biopolymers*, 2003, **72**(3), 149–161.
19 A. Průšová, D. Šmejkalová, M. Chytil, V. Velebný and J. Kučerík, An alternative DSC approach to study hydration of hyaluronan, *Carbohydr. Polym.*, 2010, **82**(2), 498–503.
20 S. Lee, S. Kim, J. Park and J. Y. Lee, Universal surface modification using dopamine-hyaluronic acid conjugates for anti-biofouling, *Int. J. Biol. Macromol.*, 2020, **151**, 1314–1321.
21 T. Euppayo, V. Punyapornwithaya, S. Chomdej, S. Ongchai and K. Nganvongpanit, Effects of hyaluronic acid combined with anti-inflammatory drugs compared with hyaluronic acid alone, in clinical trials and experiments in osteoarthritis: a systematic review and meta-analysis, *BMC Musculoskeletal Disord.*, 2017, **18**, 1–14.
22 P. Andre, Hyaluronic acid and its use as a" rejuvenation" agent in cosmetic dermatology, in *Seminars in cutaneous medicine and surgery*, 2004, vol. 23, pp. 218–222.
23 G. Kogan, L. Šoltés, R. Stern and P. Gemeiner, Hyaluronic acid: a natural biopolymer with a broad range of biomedical and industrial applications, *Biotechnol. Lett.*, 2007, **29**, 17–25.
24 A. Borzacchiello, L. Russo, B. M. Malle, K. Schwach-Abdellaoui and L. Ambrosio, Hyaluronic acid based hydrogels for regenerative medicine applications, *BioMed Res. Int.*, 2015, **2015**, 871218.
25 C. Branca, S. Magazu, G. Maisano, F. Migliardo, P. Migliardo and G. Romeo, Hydration study of PEG/water mixtures by quasi elastic light scattering, acoustic and rheological measurements, *J. Phys. Chem. B*, 2002, **106**(39), 10272–10276.
26 K. Bjugstad, D. Redmond Jr., K. Lampe, D. Kern, J. Sladek Jr. and M. Mahoney, Biocompatibility of PEG-based hydrogels in primate brain, *Cell Transplant.*, 2008, **17**(4), 409–415.
27 C. Caddeo, L. Pucci, M. Gabriele, C. Carbone, X. Fernàndez-Busquets, D. Valenti, R. Pons, A. Vassallo, A. M. Fadda and M. Manconi, Stability, biocompatibility and antioxidant activity of PEG-modified liposomes containing resveratrol, *Int. J. Pharm.*, 2018, **538**(1–2), 40–47.
28 M. Catauro, F. Bollino, F. Papale, C. Ferrara and P. Mustarelli, Silica–polyethylene glycol hybrids synthesized by sol–gel: Biocompatibility improvement of titanium implants by coating, *Mater. Sci. Eng., C*, 2015, **55**, 118–125.
29 Y. Inada, M. Furukawa, H. Sasaki, Y. Kodera, M. Hiroto, H. Nishimura and A. Matsushima, Biomedical and biotechnological applications of PEG-and PM-modified proteins, *Trends Biotechnol.*, 1995, **13**(3), 86–91.
30 S. R. Kane, P. D. Ashby and L. A. Pruitt, Characterization and tribology of PEG–like coatings on UHMWPE for total hip replacements, *J. Biomed. Mater. Res., Part A*, 2010, **92**(4), 1500–1509.
31 D. Zeini, J. C. Glover, K. D. Knudsen and B. Nyström, Influence of Lysine and TRITC Conjugation on the Size and Structure of Dextran Nanoconjugates with Potential for Biomolecule Delivery to Neurons, *ACS Appl. Bio Mater.*, 2021, **4**(9), 6832–6842.
32 M. Zink, K. Hotzel, U. S. Schubert, T. Heinze and D. Fischer, Amino Acid–Substituted Dextran–Based Non–Viral Vectors for Gene Delivery, *Macromol. Biosci.*, 2019, **19**(8), 1900085.
33 M. G. Bauer, K. Baglo, L. Reichert, J. Torgerson and O. Lieleg, Comparing the Resilience of Macromolecular Coatings on Medical-Grade Polyurethane Foils, *Surf. Interfaces*, 2023, 103231.

34 M. Nishino, I. Matsuzaki, F. Y. Musangile, Y. Takahashi, Y. Iwahashi, K. Warigaya, Y. Kinoshita, F. Kojima and S.-I. Murata, Measurement and visualization of cell membrane surface charge in fixed cultured cells related with cell morphology, *PLoS One*, 2020, **15**(7), e0236373.

35 B. J. Huang, J. C. Hu and K. A. Athanasiou, Cell-based tissue engineering strategies used in the clinical repair of articular cartilage, *Biomaterials*, 2016, **98**, 1–22.

36 R. R. Asawa, J. C. Belkowski, D. A. Schmitt, E. M. Hernandez, A. E. Babcock, C. K. Lochner, H. N. Baca, C. M. Rylatt, I. S. Steffes and J. J. VanSteenburg, Transient cellular adhesion on poly (ethylene-glycol)-dimethacrylate hydrogels facilitates a novel stem cell bandage approach, *PLoS One*, 2018, **13**(8), e0202825.

37 S. Cai, C. Wu, W. Yang, W. Liang, H. Yu and L. Liu, Recent advance in surface modification for regulating cell adhesion and behaviors, *Nanotechnol. Rev.*, 2020, **9**(1), 971–989.

38 Y. M. Chen, R. Ogawa, A. Kakugo, Y. Osada and J. P. Gong, Dynamic cell behavior on synthetic hydrogels with different charge densities, *Soft Matter*, 2009, **5**(9), 1804–1811.

39 W. Mubarok, K. C. M. L. Elvitigala, M. Nakahata, M. Kojima and S. Sakai, Modulation of cell-cycle progression by hydrogen peroxide-mediated cross-linking and degradation of cell-adhesive hydrogels, *Cells*, 2022, **11**(5), 881.

40 D. Fan, B. Miller Naranjo, S. Mansi, P. Mela and O. Lieleg, Dopamine-Mediated Biopolymer Multilayer Coatings for Modulating Cell Behavior, Lubrication, and Drug Release, *ACS Appl. Mater. Interfaces*, 2023, **15**(31), 37986–37996.

41 D. Bhatnagar, K. Dube, V. B. Damodaran, G. Subramanian, K. Aston, F. Halperin, M. Mao, K. Pricer, N. S. Murthy and J. Kohn, Effects of terminal sterilization on PEG–based bioresorbable polymers used in biomedical applications, *Macromol. Mater. Eng.*, 2016, **301**(10), 1211–1224.

42 M. Marczynski, B. N. Balzer, K. Jiang, T. M. Lutz, T. Crouzier and O. Lieleg, Charged glycan residues critically contribute to the adsorption and lubricity of mucins, *Colloids Surf., B*, 2020, **187**, 110614.

43 B. Winkeljann, M. G. Bauer, M. Marczynski, T. Rauh, S. A. Sieber and O. Lieleg, Covalent Mucin Coatings Form Stable Anti–Biofouling Layers on a Broad Range of Medical Polymer Materials, *Adv. Mater. Interfaces*, 2020, **7**(4), 1902069.

44 B. Winkeljann, P. M. A. Leipold and O. Lieleg, Macromolecular coatings enhance the tribological performance of polymer-based lubricants, *Adv. Mater. Interfaces*, 2019, **6**(16), 1900366.

